Diverse Resistance Mechanisms to the Third-Generation ALK Inhibitor Lorlatinib in ALK-Rearranged Lung Cancer

Gonzalo Recondo[1,2], Laura Mezquita[3], Francesco Facchinetti[1,2], David Planchard[3], Anas Gazzah[4], Ludovic Bigot[1,2], Ahsan Z. Rizvi[1,2], Rosa L. Frias[1,2], Jean Paul Thiery[5,6,7,8,9], Jean-Yves Scoazec[2,10,11], Tony Sourisseau[1,2], Karen Howarth[12], Olivier Deas[13], Dariia Samofalova[14,15], Justine Galissant[1,2], Pauline Tesson[1,2], Floriane Braye[1,2], Charles Naltet[3], Pernelle Lavaud[3], Linda Mahjoubi[4], Aurélie Abou Lovergne[2,16], Gilles Vassal[16], Rastilav Bahleda[4], Antoine Hollebecque[4], Claudio Nicotra[4], Maud Ngo-Camus[4], Stefan Michiels[17], Ludovic Lacroix[1,2,10,11], Catherine Richon[10], Nathalie Auger[11], Thierry De Baere[18], Lambros Tselikas[18], Eric Solary[19], Eric Angevin[4], Alexander M. Eggermont[3], Fabrice Andre[1,2,3], Christophe Massard[1,2,4], Ken A. Olaussen[1,2], Jean-Charles Soria[1,2,4], Benjamin Besse[1,2,3], and Luc Friboulet[1,2]

ABSTRACT

Purpose: Lorlatinib is a third-generation anaplastic lymphoma kinase (ALK) tyrosine kinase inhibitor with proven efficacy in patients with ALK-rearranged lung cancer previously treated with first- and second-generation ALK inhibitors. Beside compound mutations in the *ALK* kinase domain, other resistance mechanisms driving lorlatinib resistance remain unknown. We aimed to characterize the mechanisms of resistance to lorlatinib occurring in patients with *ALK*-rearranged lung cancer and design new therapeutic strategies in this setting.

Experimental Design: Resistance mechanisms were investigated in 5 patients resistant to lorlatinib. Longitudinal tumor biopsies were studied using high-throughput next-generation sequencing. Patient-derived models were developed to characterize the acquired resistance mechanisms, and Ba/F3 cell mutants were generated to study the effect of novel *ALK* compound mutations. Drug combi-

natory strategies were evaluated *in vitro* and *in vivo* to overcome lorlatinib resistance.

Results: Diverse biological mechanisms leading to lorlatinib resistance were identified. Epithelial–mesenchymal transition (EMT) mediated resistance in two patient-derived cell lines and was susceptible to dual SRC and ALK inhibition. We characterized three *ALK* kinase domain compound mutations occurring in patients, L1196M/D1203N, F1174L/G1202R, and C1156Y/G1269A, with differential susceptibility to ALK inhibition by lorlatinib. We identified a novel bypass mechanism of resistance caused by *NF2* loss-of-function mutations, conferring sensitivity to treatment with mTOR inhibitors.

Conclusions: This study shows that mechanisms of resistance to lorlatinib are diverse and complex, requiring new therapeutic strategies to tailor treatment upon disease progression.

Introduction

The anaplastic lymphoma kinase (ALK) is a member of the family of insulin-like tyrosine kinase receptors involved in the oncogenesis of several tumor types (1). *ALK* gene rearrangements occur in 3%–6% of lung adenocarcinomas (2, 3). Patients diagnosed with *ALK*-rearranged lung cancer benefit from treatment with ALK tyrosine kinase inhibitors (TKI; ref. 4).

Lorlatinib is a potent third-generation ALK inhibitor able to overcome resistance to first- and second-generation ALK inhibitors, including those mediated by the G1202R mutation and has marked activity on brain metastasis (5). Clinical responses with lorlatinib were observed in 39% of patients previously treated with two or more ALK inhibitors and median progression-free survival (PFS) was 6.9 months (6, 7). Nevertheless, as with first- and second-

[1]INSERM U981, Gustave Roussy Cancer Campus, Villejuif, France. [2]Université Paris-Saclay, Paris, France. [3]Department of Medical Oncology, Gustave Roussy Cancer Campus, Villejuif, France. [4]Drug Development Department (DITEP), Gustave Roussy Cancer Campus, Villejuif, France. [5]Yong Loo Lin School of Medicine, National University of Singapore, Republic of Singapore. [6]Institute of Biomedicine and Health, Chinese Academy of Science, Beijing, P.R. China. [7]CCBIO, Department of Clinical Medicine, Faculty of Medicine and Dentistry, The University of Bergen, Bergen, Norway. [8]Department of Clinical Oncology, Li Ka Shing Faculty of Medicine, Hong Kong University, Hong Kong. [9]CNRS UMR 7057 Matter and Complex Systems, University Paris Denis Diderot, Paris, France. [10]Experimental and Translational Pathology Platform (PETRA), Genomic Platform-Molecular Biopathology Unit (BMO) and Biological Resource Center, AMMICA, INSERM US23/CNRS UMS3655, Gustave Roussy Cancer Campus, Villejuif, France. [11]Department of Medical Biology and Pathology, Gustave Roussy Cancer Campus, Villejuif, France. [12]Inivata, Granta Park, United Kingdom. [13]XenTech, Evry, France. [14]Life Chemicals Inc., Ontario, Canada. [15]Institute of Food Biotechnology and Genomics NAS of Ukraine, Kyiv, Ukraine. [16]Department

of Clinical Research, Gustave Roussy Cancer Campus, Villejuif, France. [17]Department of Biostatistics and Epidemiology, Gustave Roussy Cancer Campus, Villejuif, France. [18]Department of Interventional Radiology, Gustave Roussy Cancer Campus, Villejuif, France. [19]Department of Hematology, Gustave Roussy Cancer Campus, Villejuif, France.

Translational Relevance

Diverse resistance mechanisms were identified using next-generation sequencing and cell lines established from patients with anaplastic lymphoma kinase (ALK)-rearranged non–small cell lung cancer treated with lorlatinib. These mechanisms include epithelial-to-mesenchymal transition susceptible to combined ALK/SRC inhibition, ALK compound mutations, and a novel bypass mechanism, mediated by NF2 loss and overcome by mTOR inhibition. This study provides further evidence on the complexity of lorlatinib resistance and new treatment strategies to overcome resistance in selected scenarios.

generation ALK inhibitors, resistance to lorlatinib treatment invariably occurs.

The spectrum of biological mechanisms driving lorlatinib resistance in patients remains to be elucidated. It has been recently reported that the sequential acquisition of two or more mutations in the ALK kinase domain (KD), also referred as compound mutations, is responsible for disease progression in about 35% of patients treated with lorlatinib, mainly by impairing its binding to the ALK kinase domain (8).

Herein, we report the *in vitro* characterization of three resistance mechanisms detected in patients with *ALK*-rearranged lung cancer on lorlatinib, included in the prospective MATCH-R study (NCT02517892). These mechanisms include the occurrence of epithelial-to-mesenchymal transition (EMT) susceptible to combined ALK/SRC inhibition (patient MR57 and MR210), the acquisition of a novel compound mutation (G1202R/F1174L in MR144), and the preexisting L1196M/D1203N (MR347) as well as NF2-loss of function–mediated resistance overcome by mTOR inhibitors (MR135).

Materials and Methods

MATCH-R clinical trial

The MATCH-R study is a prospective single-institution trial running at Gustave Roussy Cancer Campus (Villejuif, France) aiming to identify mechanisms of resistance to targeted therapies in patients with advanced cancer (NCT02517892). Patients that achieved a partial or complete response, or stability of disease for atleast 6 months with selected targeted agents, were included in the study and underwent serial tumor biopsies. Extensive molecular tumor profiling was performed by panel-targeted next-generation sequencing (NGS; Ion torrent), whole-exome sequencing (WES), and RNA sequencing (Illumina; Integragen) as described previously (9). For WES, mean coverage was 140×.

Development of patient-derived xenografts in mice and *in vivo* pharmacologic studies

All animal procedures and studies were performed in accordance with the approved guidelines for animal experimentation by the ethics committee at University Paris Sud (Paris, France; CEEA 26, Project 2014_055_2790) following EU regulation. Fresh tumor fragments from the patients MR57, MR135, MR144, MR210, and MR347 were implanted in the subrenal capsule of 6-week-old female NOD scid gamma (NSG) or nude mice obtained from Charles River Laboratories.

Cell lines

Patient-derived cell lines [MR57 sensitive (MR57-S), MR57 resistant (MR57-R), MR135-R1, MR135-R2, and MR210] were developed from patient-derived xenograft (PDX) samples by enzymatic digestion with a tumor dissociation kit (ref. 130-095-929, Miltenyi Biotec) and mechanic degradation with the GentleMACs dissociator. Cells were cultured with DMEM/F-12 + GlutamMAX 10% FBS and 10% enriched with hydrocortisone 0.4 μg/mL, cholera toxin 8.4 ng/mL, adenine 24 μg/mL, and ROCK inhibitor 5 μmol/L (Y-27632, S1049 Selleckchem) until a stable proliferation of tumor cells was observed, as described previously (10). Culture media were then transitioned to DMEM and cultured in the presence of lorlatinib from 300 nmol/L to 1 μmol/L. The H3122 cell line harboring EML4-ALK rearrangement was cultured in RPMI 10% FBS. Parental Ba/F3 cells were purchased from DSMZ and cultured in DMEM 10% FBS in the presence of IL3 (0.5 ng/mL). Ba/F3 cells were infected with lentiviral constructs as reported previously to express the EML4-ALK variant 3 fusion with or without ALK kinase domain mutations (11). Ba/F3 cells harboring the *EML4-ALK* fusion were selected in the presence of blasticidin (21 μg/mL) and IL3 (0.5 ng/mL) until recovery, and a second selection by culturing the cells in the absence of IL3. *EML4-ALK* rearrangement and *ALK* kinase domain mutations or *NF2* mutations were confirmed on the established cell lines by Sanger sequencing.

CRISPR-based NF2 knocking out

NF2 gene knock out was performed with the CRISPR/Cas9 KO Plasmid (h) from Santa Cruz Biotechnology (sc-400504). CRISPR/Cas9 KO Plasmid (h) was transfected using Lipofectamine 3000 according to manufacturer's protocol. GFP-based cell sorting was performed for clonal selection. Single clones were screened for *NF2* gene disruption by RT-PCR followed by sequencing and Western blot analysis.

Site-directed mutagenesis

Lentiviral vectors expressing the EML4-ALK variant 3 were created using the pLenti6/V5 directional TOPO Cloning Kit (#K495510, Thermo Fisher Scientific) according to the manufacturer's instructions. Point mutations were introduced using the QuickChange XL Site-Directed Mutagenesis Kit (#200516, Agilent) according to manufacturer's protocol using the following primers:

G1269A forward (F): GAGTGGCCAAGATTGCAGACTTCGGGATGGCC
G1269A reverse (R): GGCCATCCCGAAGTCTGCAATCTTGGCCACTC
C1156Y F: GACGCTGCCTGAAGTGTACTCTGAACAGGACGAAC
C1156Y R: GTTCGTCCTGTTCAGAGTACACTTCAGGCAGCGTC
E1154K F: CTGTGAAGACGCTGCCTAAAGTGTGCTCTGAACAG
E1154K R: CTGTTCAGAGCACACTTTAGGCAGCGTCTTCACAG
F1174L F: TGTTCTGGTGGTTTAATTTGCTGATGATCAGGGCTTCC
F1174L R: GGAAGCCCTGATCATCAGCAAATTAAACCACCAGAACA
G1202R F: GCTCATGGCGGGGAGAGACCTCAAGTCC
G1202R R: GCTCATGGCGGGGAGAGACCTCAAGTCC
D1203N F: ATGGCGGGGGGAAACCTCAAGTCCTTCC
D1203N R: GGAAGGACTTGAGGTTTCCCCCCGCCAT
L1196M F: GCCCCGGTTCATCCTGATGGAGCTCATGGCGGG
L1196M R: CCCGCCATGAGCTCCATCAGGATGAACCGGGGC.

Reagents

Saracatinib (AZD0530) and vistusertib (AZD2014) were provided by AstraZeneca. Crizotinib (S1068), alectinib (S2762), brigatinib

(S8229), dasatinib (S1021), erdafitinib (S8401), Debio-1347 (S7665), lorlatinib (S7536), and entrectinib (S7998) were purchased from Selleck Chemicals.

For Western blot assays, the following antibodies were used: pALK Y1282/1283 (9687S), pALK Y1604 (3341S), ALK (3333S), pAKT (4060S), AKT (4961S), pERK (9101S), ERK (9102S), pS6 (4858S), S6 (2217S), cleaved Parp (9541S), BIM (2933S), Merlin (1288S), pPaxillin (2541S), Paxillin (2542S), Snail (3879S), and Vimentin (5741S) were purchased from Cell Signaling Technology.

For IHC assays, the following antibodies were used: ALK (6679072001), E-cadherin (790-4497), and CD31 (760-4378) purchased from Ventana; N-cadherin (M3613), Ki-67 (M7240), β-catenin (M3539), podoplanin (M3619), and CD68 (M0814) purchased from DAKO; Vimentin (790-2917) purchased from Roche; pSRC (6943S) and pMAPK (4376) purchased from Cell Signaling Technology; Glut1 (RP128-05) purchased from Clinisciences; CA-IX (NB100-417SS) purchased from Novus Biologicals, NF2/Merlin purchased from Sigma-Aldrich (HPA003097); and CD47 (M5792) purchased from Spring.

Cell viability and apoptosis assays

Cell viability assays were performed in 96-well plates using the CellTiter Glo Luminescent Cell Viability Assay (G7570, Promega). Apoptosis was measured using the Caspase-Glo 3/7 Assay (G8091, Promega).

In vivo pharmacologic studies

MR135-R2 PDX-bearing athymic nude mice were treated with vistusertib, 20 mg/kg once daily (QD) 3 days on, 4 days off; lorlatinib, 20 mg/kg QD 5 days on, 2 days off; or their combination by oral gavage. Vistusertib was resuspended in 1% Tween80 in sterile deionized water and lorlatinib in sterile deionized water pH 3.0.

Circulating tumor DNA analysis from patient's blood samples

A total of 20 mL of blood was collected in Streck BCT (Streck) or EDTA tubes and processed for DNA extraction. Molecular analysis from circulating tumor DNA (ctDNA) was performed by Inivata using amplicon-based NGS (InVisionFirst-Lung) as reported previously (12).

Actin microfilament staining with phalloidin

MR210, MR57-S, and MR57-R cells were fixed in formaldehyde and permeabilized with PBS Triton X-100 (0.05%). Blocking solution with FBS 2% and BSA 1% was used. Alexa Fluor 488 Phalloidin (8878S, Cell Signaling Technology) solution was diluted 1/200 in blocking buffer. Cells were incubated for 1 hour at room temperature, then washed with PBS, and later incubated with DAPI 1/10,000 dilution for 5 minutes. Cells were imaged with an inverted IX73 microscope (Olympus).

Allelic distribution of ALK mutations

The ALK kinase domain was amplified by PCR and amplicons were subcloned into pCR2.1-TOPO vector (Invitrogen) according to the manufacturer's protocol. Individual cDNA was sequenced by Sanger sequencing to determine the cis/trans status of mutations.

Modeling tumor clonal evolution

Paired-end RNA sequencing data for MR144 sequential biopsies was mapped against the human genome version "hg19" through Burrows-Wheeler Aligner (13). The resulting Sequence Alignment Map (SAM) was converted into binary version BAM files. PCR duplicates identified in BAM files were removed with "samtools

fixmate." Realign Target Creator and realigner of GATK were used to check and realign the sorted BAM files with predefined BED files for indels. The GATK-Base Recalibrator was used to generate tables for user-specified covariates and GATK-MuTect2 was used to calculate variant allelic frequency (VAF). Computed VAFs of different time-points were adjusted according to tumor cell percentages and subjected to R-SciClone clustering analysis (14). The phylogeny of subclonal tumor evolution was determined using R-clonevol (15) and visualized with R-fishplot (16).

Computational modeling of ALK

All molecules for reconstruction and analysis of human ALK kinases were taken from RCSB Protein Data Bank (PDB) and information obtained from UniProtKB database (17, 18). Full three-dimensional models of ALK domains were built using I-TASSER server (19). Structure and assembling of polypeptide chains were analyzed using data of SCOP database (20). The secondary structure of ALK domain was verified on the basis of self-optimized prediction method with alignment (SOPMA). Also, BioLuminate (Schrödinger) was used as a method for evaluating the role of amino acid mutations (21, 22). Geometry optimization and stability of reconstructed models were predicted on the basis of results of molecular dynamics (MD) simulations. MD simulations were performed in an aqueous environment, using CHARMM force field and GROMACS 5.1.4 program package (23, 24). Each protein was solvated, optimized (10,000 steps steepest descent/conjugant gradient algorithms), equilibrated (30,000 steps), and relaxed during a free MD in water environment (50 ns). Lorlatinib topology was generated with online SwissParam tool (25). MD results were evaluated by RMSD, values of conformational energies, and radius of gyration. Assessment of the amino acid composition, visualization, and structure analysis were performed in PyMOL and BIOVIA DS Visualizer. CCDC GOLD 5.2.2 suite (www.ccdc.cam.ac.uk) was used for final exhaustive docking of hit compounds. The major part of docking options was turned on by default; however, ChemScore function, which relies on the internal energy calculation, was altered to ASP algorithm (26). We kept GoldScore function as a primary function as it provides best conformational search analysis. https://www.lifechemicals.com.

Results

Resistance mechanisms to ALK TKI from MATCH-R clinical trial

From January 2015 to January 2019, 14 patients with ALK-rearranged tumors progressing on ALK TKI were included in the MATCH-R study. Four patients were excluded from the analysis due to inadequate biopsies for molecular profiling (Fig. 1).

Among the 8 patients with ALK-rearranged lung adenocarcinoma, tumor biopsies were obtained upon progression to crizotinib (n = 1), ceritinib (n = 3), and lorlatinib (n = 4; Table 1). NGS analysis of tumor biopsies from patients treated with crizotinib and ceritinib revealed the presence of secondary ALK kinase domain mutations in three cases (G1269A, L1196M/D1203N, and F1174L) and a NOTCH1 variant of unknown significance in one additional case (Table 1). The ceritinib-resistant patient with the compound mutation L1196M/D1203N (MR347) experienced primary resistance to lorlatinib and is therefore characterized here as an additional lorlatinib resistance mechanism. Among the 4 patients with ALK-rearranged lung cancer with acquired resistance to lorlatinib, ALK compound mutations were observed in two cases (C1156Y/G1269A for patient MR57 and G1202R/F1174L for patient MR144). Off-target mutations in NF2 were encountered in two different temporospatial biopsies from patient MR135 obtained while
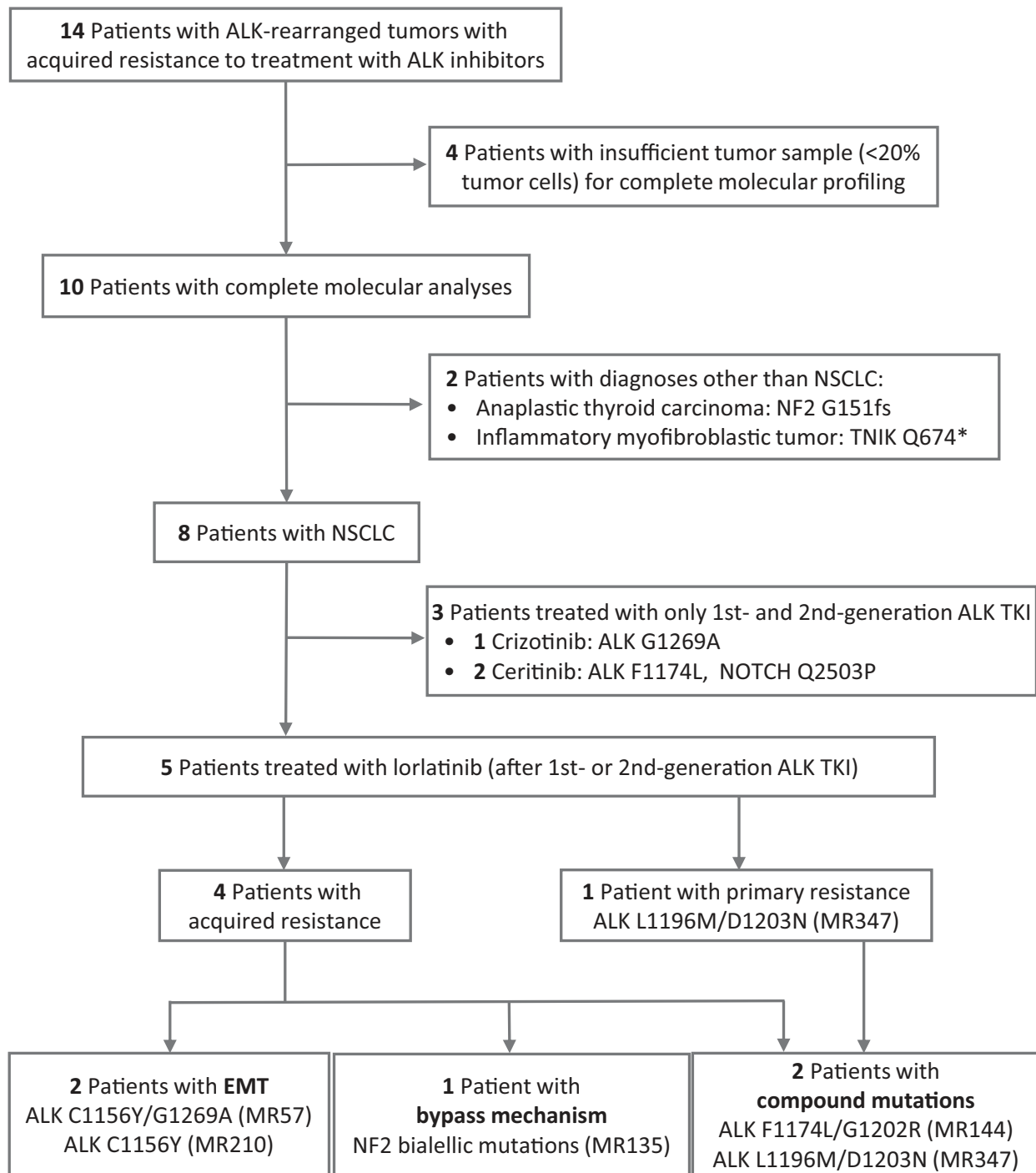
Figure 1.
Summary of ALK-rearranged patients included in the MATCH-R study.

on treatment with lorlatinib. The first biopsy was from an oligo-progressive lung lesion after 7 months of lorlatinib treatment that was treated with stereotactic radiation, and the second biopsy was obtained at the time of systemic progression from an adrenal metastasis after additional 8 months of treatment with lorlatinib. A single *ALK* C1156Y kinase domain mutation was found in 1 patient (MR210) after

progression to lorlatinib, without evidence of additional genetic alterations. The *ALK* C1156Y mutation is known to confer resistance to crizotinib and ceritinib, but remains sensitive to lorlatinib, as reported previously in preclinical studies (5). Thus, the C1156Y mutation is not likely to be responsible for lorlatinib resistance in this case. Patient-derived cell lines were developed from patients

Table 1. Clinical and molecular features of patients with tumor molecular profiling on biopsies obtained upon resistance to ALK inhibitors in the MATCH-R study.

ID	Diagnosis	Previous ALK TKI	NGS at progression to previous line of ALK TKI	Line of ALK TKI inclusion	ALK TKI MATCH-R inclusion	Response (RECIST) PFS	Targeted sequencing	WES/RNA sequencing	Putative resistance mechanism
MR 39	LUAD	Crizotinib	No	2	Ceritinib	PR 14 months	No detectable alterations	*NOTCH1*: p.Q2503P	Unknown
MR 57	LUAD	Crizotinib	No	2	Lorlatinib	PR 7 months	*ALK*: p.C1156Y/G1269A	*ALK*: p.C1156Y/G1269A	EMT
MR 135	LUAD	Crizotinib	*NF2* c.886IG>A *NF2* p.S288*	2	Lorlatinib	PR 15 months	*PTPN11*: p.S502L *TP53*: p.R273P	*NF2*: p.K543N *NF2* c.886-1G>A	NF2 bypass
MR 143	ATC	No	NAP	1	Crizotinib	SD 5 months	*TP53*: p.E285*	*TNIK*: p.Q674*	Unknown
MR 144	LUAD	Crizotinib Ceritinib Brigatinib	*ALK*: p.E1154K+p.G1202R N/A *ALK*: p.G1202R	4	Lorlatinib	PR 4 months	*ALK*: p.G1202R/F1174L	*ALK*: p.G1202R/F1174L	*ALK*: p.G1202R/F1174L
MR 154	MIT	Crizotinib	No	2	Ceritinib	SD 26 months	No detectable alterations	*NF2*: p.G151fs	NF2 bypass
MR 176	LUAD	No	NAP	1	Crizotinib	PR 30 months	No detectable alterations	*ALK*: p.G1269A	*ALK*: p.G1269A
MR 210	LUAD	Crizotinib Ceritinib	No	3	Lorlatinib	PR 16 months	*ALK*: p.C1156Y	*ALK*: p.C1156Y	EMT
MR 344	LUAD	Crizotinib	No	2	Ceritinib	PR 4 months	*ALK*: p.F1174L	*ALK*: p.F1174L; PIK3CB: p.E1051K	*ALK*: p.F1174L
MR 347	LUAD	Crizotinib	*ALK*: p.L1196M	2	Ceritinib	PR 5 months	ctDNA *ALK*: p.L1196M/D1203N	*ALK*: p.L1196M	*ALK*: p.L1196M/D1203N
	LUAD			3	Lorlatinib	PD	N/A	N/A	N/A

Abbreviations: ATC, anaplastic thyroid carcinoma; LUAD, lung adenocarcinoma; MIT, myofibroblastic inflammatory tumor; NAP, not applicable; N/A, not available.

MR57, MR135, and MR210. Biological processes driving tumor resistance to lorlatinib were further explored using patient-derived cell lines.

Epithelial–mesenchymal transition mediates lorlatinib resistance

A 59-year-old male was diagnosed with a metastatic *ALK*-rearranged lung adenocarcinoma (**Fig. 2A**). The patient received first-line treatment crizotinib achieving a partial response and a PFS of 4.2 months. At the time of disease progression to crizotinib, neither tumor nor plasma was available. The patient received sequential second-line treatment with lorlatinib at 75 mg daily achieving a partial response (-78% per RECIST criteria). After 6.9 months, disease progression was observed, the patient was included in the MATCH-R trial (MR57) and a lung biopsy on the progressing primary site was performed.

Targeted NGS, WES, and RNA sequencing showed the presence of both C1156Y and G1269A *ALK* mutations and the *EML4-ALK* variant 3 rearrangement (V3). cDNA Topo-TA cloning and sequencing of the *ALK* kinase domain evidenced that both mutations were present in the same allele (compound mutation).

A PDX model was established directly from a biopsy and a cell line (MR57-S) was derived from the PDX, with a total elapsed time from the tumor biopsy to cell line establishment of 6 months. Cell survival assays showed that the patient-derived cell line was sensitive to lorlatinib treatment (MR57-S), with an IC_{50} of 50 nmol/L, suggesting that the C1156Y/G1269A compound mutation was not likely responsible for lorlatinib resistance (Supplementary Fig. S1A). It remains to be elucidated whether lorlatinib withdrawal during the time of PDX development and cell line establishment could have influenced the observed sensitivity of the MR57-S cell line. To further study the effect of this *ALK* compound mutation on ALK inhibitors' sensitivity, we developed Ba/F3-engineered cells to express the EML4-ALK V3 with G1269A, C1156Y, or compound C1156Y/G1269A mutations. Ba/F3 cells expressing EML4-ALK with the compound mutations were less sensitive to lorlatinib (IC_{50}: 53 nmol/L) than Ba/F3 cell expressing the C1156Y (IC_{50}: 2.5 nmol/L) or G1269A (IC_{50}: 18 nmol/L) single mutations (Supplementary Fig. S1B). However, the doses required to induce cell death in these models were within the range of lorlatinib sensitivity, being lower than those required to target the G1202R mutation, known to be susceptible to lorlatinib inhibition in patients (5, 6). The C1156Y/G1269A compound mutation conferred resistance to crizotinib, alectinib, and entrectinib, but not to brigatinib, when tested *in vitro* (Supplementary Fig. S1C).

The MR57-S cell line was exposed to incremental concentrations of lorlatinib until the tumor cells developed resistance, achieving stable growth at a dose of 300 nmol/L. The MR57-R cell line showed high levels of resistance to lorlatinib (IC_{50}: 7.8 µmol/L; Supplementary Fig. S1A). Sequencing of the ALK kinase domain in both MR57-S and MR57-R cells showed the presence of the C1156Y and G1269A mutations. MR57-R cells did not acquire any additional *ALK* kinase domain mutations during exposure to lorlatinib.

Immunoblot analysis of MR57-S and MR57-R cells treated with incremental doses of lorlatinib showed that ALK inhibition resulted in inhibition of ERK, AKT, and S6 phosphorylation and induction of apoptosis in MR57-S cells (**Fig. 2B**). In contrast, MR57-R cells maintained high levels of ERK, AKT, and S6 phosphorylation, with lower levels of apoptosis. This is in line with the occurrence of an off-target mechanism of resistance (i.e., the activation of a bypass track).

Because MR57-S and MR57-R cells had markedly different morphologies, we assessed the differential expression of EMT markers. Immu-

noblot analysis revealed that MR57-S cells expressed high levels of E-cadherin and lacked N-cadherin and vimentin, characteristic of an epithelial phenotype. In contrast, MR57-R cells lacked E-cadherin expression and had high levels of N-cadherin, Snail and vimentin expression, characteristic features of a mesenchymal phenotype (**Fig. 2B**). RNA sequencing of the two cell lines confirmed the differential expression of EMT-related genes at the mRNA level (Supplementary Fig. S1D). Comparably, MR57-R cells had higher levels of vimentin, CDH-2 (N-cadherin), SNAIL, ZEB1, FGFR1, and TGFB1/2 mRNA expression and lower levels of EPCAM, CDH-1 (E-cadherin), and ICAM1 expression compared with MR57-S cells. In addition, we performed phalloidin staining of actin microfilaments on MR57-S and MR57-R cells. Lorlatinib-sensitive cells manifested the formation of actin rings and proliferation in clusters, distinctive of an epithelial phenotype (Supplementary Fig. S1E). In contrast, MR57-R contained actin stress fibers, which is characteristic of a mesenchymal phenotype.

To assess whether EMT features were present in the patient's tumor upon progression to lorlatinib, we compared the expression of EMT markers by IHC on precrizotinib and at the time of disease progression with lorlatinib using FFPE specimens (Supplementary Fig. S1F). EMT features were not observed in the patient's tumor specimen upon lorlatinib progression, evidenced by the expression of E-cadherin and the absence of vimentin and N-cadherin expression. Cancer cells were spatially relocated in lymphatic vessels (CD31$^+$, Podoplanin$^+$), in a hypoxic [Carbonic Anhydrase 9 (CAIX$^+$), Glucose Transporter 1 (Glut1$^+$)] and immune-evading microenvironment (CD47$^+$ and CD68 low) with sustained MAPK phosphorylation. In the absence of EMT features in the tumor biopsy, these other factors could have contributed to disease progression by limiting drug availability. Nevertheless, the onset of an EMT program upon lorlatinib exposure in patient-derived cell line supports the role of EMT in lorlatinib resistance in this model *in vitro*.

A second patient became resistant to lorlatinib without evidence of any mutation causing TKI resistance (MR210). This 58-year-old never smoker female patient with metastatic ALK-rearranged NSCLC had a benefit over four years from crizotinib treatment (**Fig. 2C**). The treatment was switched to ceritinib due to progressing bone metastasis, but ceritinib was suspended after one cycle due to toxicity. Treatment was switched to lorlatinib, achieving a response that lasted for 16 months, when oligo-progression in a bone lesion occurred. The patient was included in the MATCH-R trial (MR210) and a tumor biopsy was performed. The patient received treatment with cryoablation to the bone metastasis and currently continues to benefit from treatment with lorlatinib, ongoing for 35 months. The MR210 cell line was directly resistant to lorlatinib and similarly to MR57 displayed EMT features. Phalloidin staining confirmed the presence of actin stress fibers and the mesenchymal phenotype (**Fig. 2D**).

We evaluated the expression of EMT markers by IHC on precrizotinib and postlorlatinib FFPE specimens. While E-cadherin and N-cadherin expression were of similar intensity and percent-positive cells among both samples, we observed an increase in vimentin expression in the postlorlatinib specimen. This would suggest a partial EMT in the tumor at the time of resistance consistent with the observed EMT in the patient-derived cell line (Supplementary Fig. S1G).

Combined SRC and ALK inhibition overcome EMT-mediated lorlatinib resistance

To overcome the resistance in these models, we tested 66 pharmacologic compounds on MR57-R and MR210 cell lines in the presence or absence of lorlatinib. The SRC inhibitor saracatinib in combination with lorlatinib showed a potent synergistic effect on both
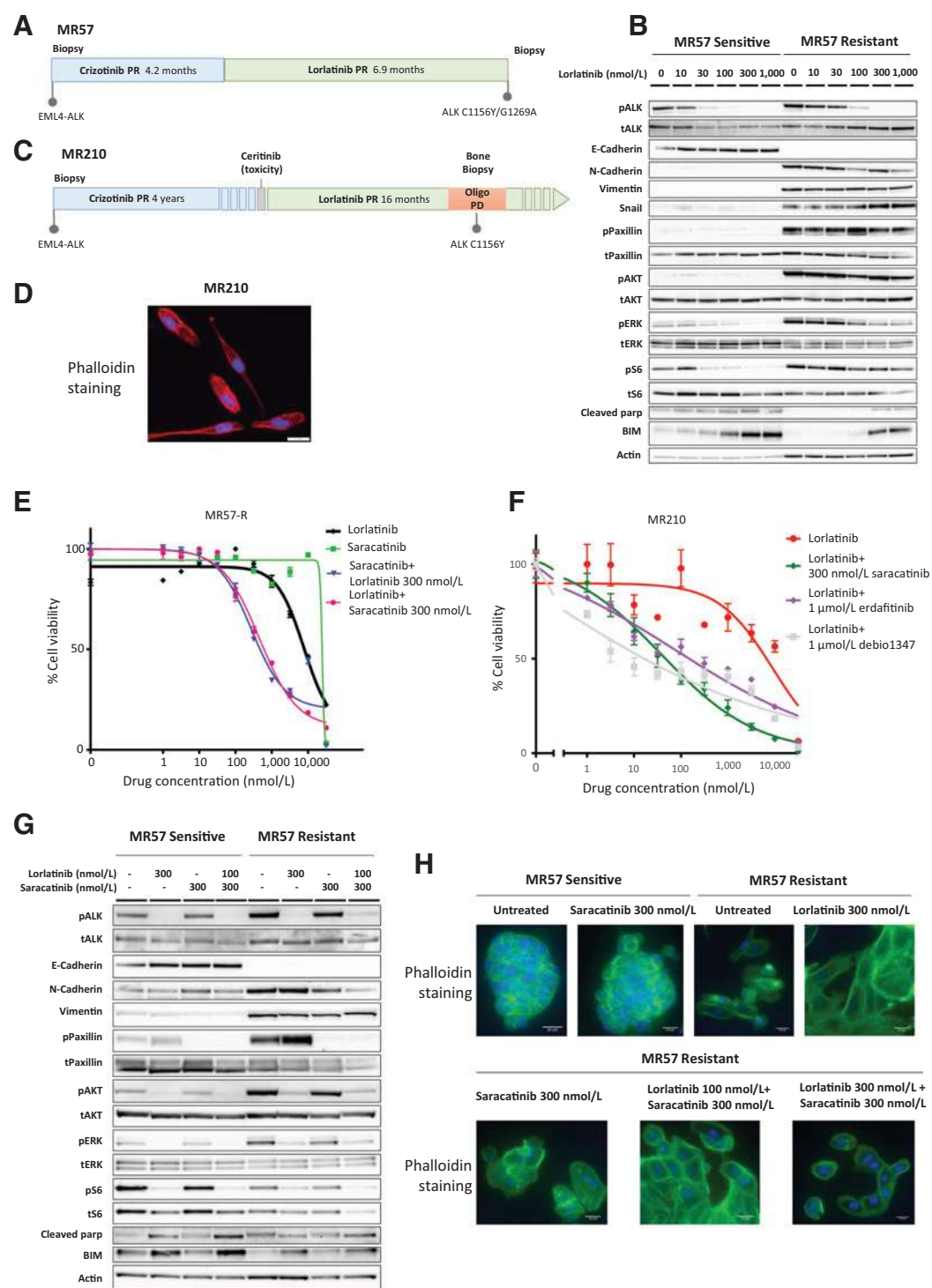
Figure 2.
SRC and ALK inhibition overcomes lorlatinib resistance mediated by EMT. **A,** Treatment course of patient MR57 (PR, partial response). **B,** MR57-S and MR57-R cells were treated with increasing concentrations of lorlatinib for 24 hours. Cell lysates were immunoblotted to detect the selected proteins. **C,** Treatment course of patient MR210 (PD, progressive disease). **D,** Phenotype of MR210 mesenchymal cells labeled with Cy3 Phalloidin and DAPI. **E,** MR57-R cells were treated with the indicated doses of lorlatinib and saracatinib alone or in combination, for 7 days. Cell viability was assessed with CellTiter Glo. **F,** MR210 cells were treated with single agents lorlatinib, saracatinib, erdafitinib, and Debio-1347 or in combination for 7 days. Cell viability was assessed with CellTiter Glo. **G,** MR57 lorlatinib-sensitive (epithelial) and -resistant (mesenchymal) cells were treated with the specified concentrations of lorlatinib and saracatinib for 24 hours. Cell lysates were probed with antibodies against the indicated proteins. **H,** Phenotypes of MR57 epithelial and mesenchymal cells labeled with Alexa Fluor 488 Phalloidin and DAPI after treatment with lorlatinib and saracatinib for 30 days.

Figure 3.
Resistance to lorlatinib mediated by ALK kinase domain compound mutations. **A,** Clinical course of patient MR144 and allelic frequencies of ALK-resistant mutations (from RNA sequencing) with sequential treatments. **B,** Fish plot illustrating the tumor clonal evolution obtained by WES analysis during treatment with ALK inhibitors. The ALK E1154K and G1202R subclones emerged independently upon resistance to crizotinib. After disease progression with brigatinib, the ALK G1202R clone predominated and the E1154K clone became undetectable. At lorlatinib resistance, a subclone emerged from the ALK G1202R clone acquiring an additional F1174L mutation. **C,** Clinical course of patient MR347. **D,** Cell survival assay of Ba/F3 models with the indicated ALK single and the F1174L/G1202R compound mutations treated with lorlatinib for 48 hours. **E,** Cell survival assay of Ba/F3 models with the indicated ALK single and the L1196M/D1203N compound mutations treated with lorlatinib for 48 hours. **F,** ALK and downstream kinase phosphorylation in Ba/F3-mutated cells treated with the indicated concentrations of lorlatinib for 3 hours. **G,** Direct comparison of ALK phosphorylation in Ba/F3 models by immunoblotting of cell lysates after 3-hour treatment with lorlatinib showing higher levels of ALK phosphorylation with the F1174L/G1202R compound mutation. **H,** Visual representation of aligned wild-type (green) and F1174L/G1202R–mutated (brown) ALK structures in complex with lorlatinib.
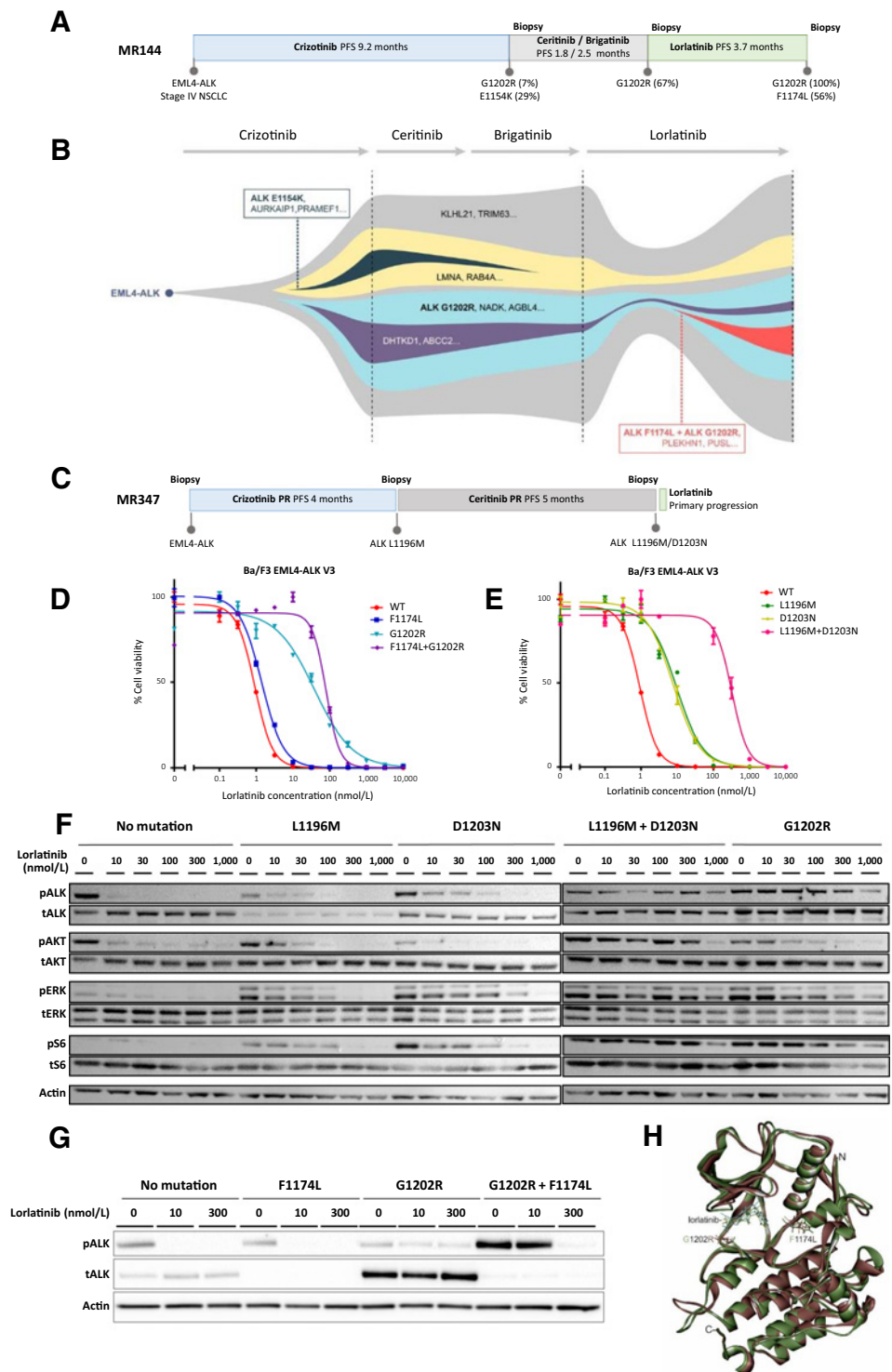
mesenchymal cell lines (**Fig. 2E** and **F**). No cytotoxic effect was observed with saracatinib on MR57-S cells with epithelial features (Supplementary Fig. S1H). In concordance, a synergistic cytotoxic effect was observed in mesenchymal cells treated with dasatinib (another SRC inhibitor) and lorlatinib (Supplementary Fig. S1I) and not in the epithelial cells (Supplementary Fig. S1J). Interestingly, FGFR inhibitors also sensitized MR210 cells to lorlatinib treatment (and to a

lower extent in MR57, data not shown) as it has recently been shown for EGFR-mutant NSCLC (**Fig. 2F**; ref. 17).

Immunoblot analysis showed that MR57-R mesenchymal cells had higher levels of paxillin phosphorylation (a surrogate for SRC activation), compared with the epithelial MR57-S cells, suggesting that SRC was driving EMT in this model, as reported previously (ref. 18; **Fig. 2B** and **G**). Consistently, treatment with saracatinib and lorlatinib
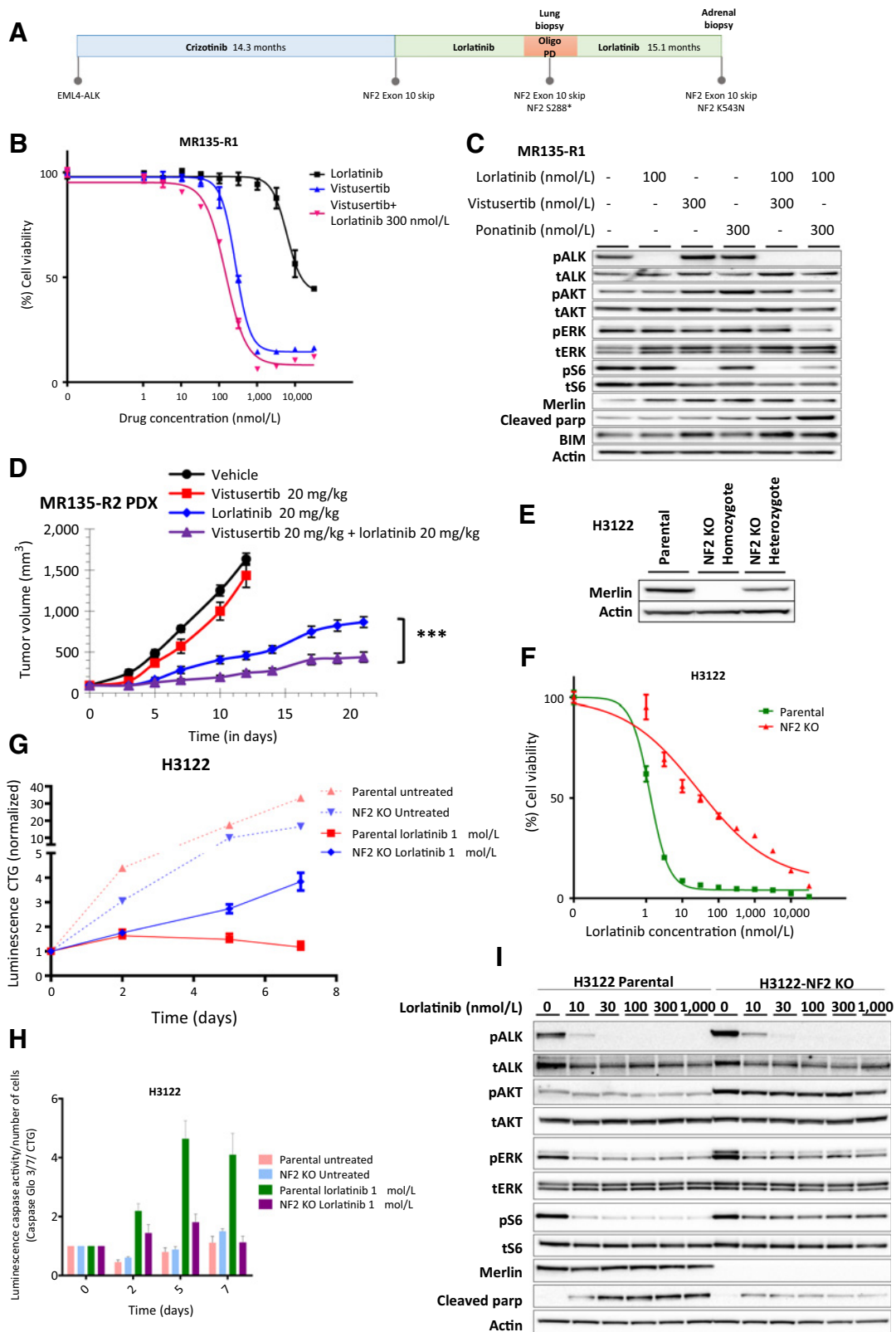
inhibited ERK, AKT, and S6 phosphorylation in MR57-R cells, which translated in a mild increase in the expression of apoptosis markers such as cleaved PARP and BIM (**Fig. 2G**).

To study whether the cytotoxic effect of combining SRC and ALK inhibition could be due to a reversion of the mesenchymal state to an epithelial phenotype, we exposed MR57-R cells to 30 days of treatment with lorlatinib, saracatinib or their combination. We observed a partial reversion in E-cadherin expression in MR57-R cells treated with saracatinib (Supplementary Fig. S1K). This effect was not observed when saracatinib was combined with lorlatinib. This suggests that continued exposure of MR57-R cells to lorlatinib can induce death in cells undergoing partial EMT reversal. Accordingly, we performed actin microfilament staining and observed that cells treated with saracatinib alone exhibited lower levels of actin stress fibers and increased formation of actin rings (**Fig. 2H**), suggesting that SRC inhibition can promote a partial EMT reversal in the long term.

Novel lorlatinib-resistant ALK compound mutations

A 58-year-old nonsmoker female was diagnosed with metastatic *ALK*-rearranged lung adenocarcinoma. The patient achieved a partial response with a 9.2 months PFS on first-line treatment with crizotinib (**Fig. 3A**). At disease progression, the patient was enrolled in the MATCH-R study (MR144). RNA sequencing confirmed the EML4-ALK V3 fusion and showed the presence of the *ALK* kinase domain–resistant mutation G1202R (VAF: 7%) and an unreported E1154K variant (VAF: 29%) on different alleles (Supplementary Fig. S2A). Amplicon-based NGS analysis of ctDNA also detected the G1202R and a I1268V mutation, but not the E1154K variant (Supplementary Fig. S2B). Because lorlatinib was not available at that time, the patient received a short course of ceritinib treatment with rapid disease progression, and treatment was switched to brigatinib. A mixed response was observed with the occurrence of new lesions after 2.5 months of treatment. A second biopsy was performed and only the G1202R mutation was detected at a higher allelic frequency (VAF: 67%). The patient started lorlatinib treatment but the benefit lasted only 3.7 months. A third biopsy was performed, and RNA sequencing showed the presence of both, a G1202R mutation (VAF: 100%) and a F1174L mutation (VAF: 56%) confirmed to be *in cis* by TOPO-TA cloning and sequencing of the ALK kinase domain (Supplementary Fig. S2C). This was consistent with ctDNA sequencing that showed a rise in G1202R detection and the appearance of the F1174L mutation. Interestingly, ctDNA analysis detected four additional cooccurring *ALK* kinase mutations, not detected in the biopsy: C1156Y, G1269A, S1206F, and T1151M (Supplementary Fig. S2B). Solely, the G1202R/S1206F mutations were confirmed to be in the same read (*cis*) with amplicon-based NGS. C1156Y and T1151M were confirmed to be *in trans,* but due to the size of the amplicons covering the ALK kinase domain, the allelic distribution of the other mutations could not be

assessed by this method. These other ALK KD mutations detected with ctDNA were not found in the sequencing analysis of the tumor biopsy, reflecting that these mutations could arise from polyclonal tumor cell subpopulations absent in the tumor biopsy.

To further characterize the clonal evolution on sequential ALK inhibitors, a FishPlot model was generated from WES compiling the three sequential patient biopsies (**Fig. 3B**). While no *ALK*-resistant mutation was detected prior to ALK TKI, multiple clones emerged at crizotinib resistance including a G1202R carrying cell population and an E1154K–mutated population. Subsequent treatments with second-generation ALK TKIs led to the disappearance of the E1154K population and the persistence of the G1202R carrying cells. Finally, at disease progression on lorlatinib, we observed an enrichment of the G1202R-mutated tumor cell population and the appearance of the F1174L mutation within this population. This case illustrates the tumor cell population dynamics when exposed to different generations of ALK TKI, in accordance with the previously described sequential acquisition of *ALK* kinase domain mutations *in cis* (8).

A 40-year-old male patient with metastatic *ALK*-rearranged lung cancer received crizotinib for 4 months (**Fig. 3C**). The patient was included in the MATCH-R trial (MR347), and tissue and ctDNA NGS detected the *ALK* gatekeeper L1196M mutation, previously known to confer resistance to crizotinib (19). The patient received ceritinib for 5 months and a second tumor biopsy was obtained from a progressive lung lesion. Targeted NGS, WES, and RNA sequencing from the tissue detected only the *ALK* L1196M mutation. ctDNA NGS further detected the presence of a solvent front D1203N mutation, present *in cis* with the L1196M, revealing a sequential development of L1196M/D1203N compound mutation. The treatment was then switched to lorlatinib but disease progression was immediately documented, proving primary resistance to lorlatinib.

Lorlatinib activity against ALK compound mutations

We generated Ba/F3 cells expressing the EML4-ALK fusion with single mutations E1154K, F1174L, G1202R, L1196M, D1203N, and the G1202R/F1174L, L1196M/D1203N compound mutations. Ba/F3 cells were treated with crizotinib, alectinib, brigatinib, entrectinib, and lorlatinib to test the differential effect of these mutations on the sensitivity to ALK inhibitors. The E1154K mutation did not confer resistance to any ALK TKI (Supplementary Fig. S2D). Its selection on crizotinib treatment remains, therefore, to be elucidated. While the F1174L mutation did not confer resistance to lorlatinib, high concentrations of lorlatinib were required to induce a cytotoxic effect on EML4-ALK^{G1202R} and EML4-ALK$^{G1202R/F1174L}$ expressing cells (5). Slightly higher concentrations of lorlatinib were required to induce cell death in Ba/F3 cells expressing EML4-ALK$^{G1202R/F1174L}$ (IC$_{50}$: 123 nmol/L) compared with cells expressing EML4-ALK^{G1202R} (IC$_{50}$: 83 nmol/L; **Fig. 3D**), which could be

Figure 4.
NF2 loss of function mediates resistance to lorlatinib. **A,** Clinical course of patient MR135 and mutational profile of samples obtained on lorlatinib progression (PD, progressive disease). **B,** Cell survival assay assessed with CellTiter Glo of MR135 lorlatinib-resistant cells from biopsy 1 (MR135-R1) treated for 7 days with the indicated concentrations of lorlatinib and vistusertib (AZD2014) alone or in combination. **C,** Immunoblot analysis from cell lysates of MR135-R1 treated for 24 hours with the specified doses of lorlatinib, vistusertib (AZD2014), and ponatinib alone or in combination using indicated antibodies. **D,** Athymic nude mice bearing MR135-R2 PDX were administered lorlatinib or vistusertib 20 mg/kg orally. Tumor volumes, mean ± SD (n = 8; ***, P < 0.001). **E,** Cell lysates from H3122 parental and H3122 cells with NF2 heterozygous deletions or homozygous deletions, generated by CRISPR-CAS9 gene editing, were immunoblotted to detect merlin expression. H3122 cells with biallelic NF2 knockout lacked merlin expression. **F,** Cell survival assay of H3122 parental and H3122 NF2 knockout (NF2 KO) cells treated with lorlatinib for 7 days. Cell survival was assessed by CellTiter Glo. **G,** Cell proliferation assay of H3122 parental and H3122 NF2 KO cells untreated and treated with lorlatinib measured at baseline, day 2, day 5, and day 7. Cell viability was assessed with CellTiter Glo. **H,** Caspase 3/7 activation (Caspase 3/7-Glo assay) relative to the number of live cells simultaneously assessed in the cell proliferation assay previously described. **I,** H3122 parental and NF2 KO cells were treated with the indicated doses of lorlatinib for 24 hours. Cell lysates were immunoblotted to detect the selected proteins.

sufficient to confer resistance in the patient. L1196M and D1203N single mutations conferred a 10-fold shift in IC_{50} compared with nonmutated cells, but the L1196M/D1203N compound mutation induced a more than 300-fold higher IC_{50} confirming the highly lorlatinib-resistant feature of this novel compound mutation (**Fig. 3E**; Supplementary Fig. S2E).

To better characterize the direct impact of those compound mutations on lorlatinib efficacy, we assessed ALK phosphorylation across these models exposed to incremental concentrations of lorlatinib. In concordance with the cell viability assay, ALK phosphorylation with the compound mutation L1196M/D1203N was maintained at high doses of lorlatinib (1 μmol/L; **Fig. 3F**). Interestingly, Ba/F3 cells expressing the other compound mutation G1202R/F1174L displayed higher basal levels of ALK phosphorylation compared with Ba/F3 cells expressing the single mutations or no secondary mutation (**Fig. 3G**; Supplementary Fig. S2F). Computational modeling of ALK further supports our finding. The F1174L mutation does not affect lorlatinib binding. However, in the context of the G1202R/F1174L compound mutation, a greater kinase stability is achieved, which could explain higher basal levels of ALK phosphorylation, and possibly contribute to resistance in this case (**Fig. 3H**).

NF2 loss of function mediates resistance to lorlatinib

A 44-year-old male was diagnosed with *ALK*-rearranged metastatic lung adenocarcinoma (**Fig. 4A**). The patient experienced disease progression after 11 months on crizotinib. The treatment was switched to lorlatinib, achieving a rapid partial response. Oligo-progressive disease occurred after 7 months of treatment with a new single lesion in the left lower lobe. The patient was included in the MATCH-R study (MR135), a biopsy of the lesion was performed and stereotactic radiotherapy (50 Gy) treatment was applied. Targeted NGS and WES of the biopsy revealed both, a *NF2* S288* nonsense mutation and a *NF2* splicing site mutation (NM_000268.3:c.886-1G>A). A PDX model was developed from this first site of progression (R1) and a patient-derived cell line was established (MR135-R1).

After 8 months of lorlatinib treatment, multiple new lesions appeared, achieving a total benefit of lorlatinib treatment for 15 months. A biopsy of the right adrenal gland was performed confirming the presence of *ALK*-rearranged lung adenocarcinoma. Interestingly, WES and RNA sequencing of this biopsy showed the same splicing site mutation (NM_000268.3:c.886-1G>A), coexisting with a new *NF2* K543N mutation. A second PDX model was developed and a second lorlatinib-resistant patient-derived cell line was established (MR135-R2). Sequencing of NF2 mRNA from both cell lines revealed a 9-base pair (bp) skipping in exon 10 as a consequence of the splicing site mutation (Supplementary Fig. S3A), but the absence of the S288 nonsense mutation and no secondary ALK KD mutations. The K543N *NF2* mutation was only present in MR135-R2 in concordance with tumor biopsy sequencing results. Both the 9 bp skipping (20) and the K543N mutation were predicted to be pathogenic (cancergenomeinterpreter.org). Merlin expression was detected by Western blot analysis in the MR135-R1 cell line as well as in the pre- and postbiopsies by IHC staining, suggesting a loss of function, but not a loss of expression, mechanism of resistance (Supplementary Fig. S3B). NF2 mutations are rare events (1.5%) in lung adenocarcinoma, and do not seem to overlap with ALK rearrangements (according to cBioPortal; ref. 21).

NF2 mutations K543N and S288* were not detected in the tumor biopsy prior to lorlatinib treatment. Importantly, the *NF2* splicing site mutation was present prior to lorlatinib treatment. The acquisition of

two different second *NF2* events attests for the temporo-spatial convergence between metastatic sites. This preexisting *NF2* splicing site mutation predisposed cancer cells to resist to lorlatinib by an NF2 loss-of-function mechanism.

Targeting lorlatinib resistance mediated by NF2 loss with mTOR inhibitors

NF2 encodes the merlin protein, a key tumor suppressor implied in the regulation of the PI3K–AKT–mTOR pathway through mTOR inhibition (22). We performed a drug screen in the MR135-R1 identifying the selective dual mTOR1-2 inhibitor, vistusertib (AZD2014, AstraZeneca), and the multikinase inhibitor, ponatinib, as hits in this cell line.

Both MR135-R1 and MR135-R2 cell lines were highly sensitive to vistusertib and the combination of vistusertib and lorlatinib (**Fig. 4B**, MR135-R1; Supplementary Fig. S3C, MR135-R2). The activity of an mTOR inhibitor was confirmed by using the clinically available rapamycin analogue everolimus (Supplementary Fig. S3D). Ponatinib, a multikinase inhibitor targeting ABL, VEGR, FGFR3, PDGFRA, and RET, showed an important synergistic effect with lorlatinib in this cell line with a 57- to 80-fold IC_{50} reduction with the combination compared with lorlatinib single agent (Supplementary Fig. S3E). However, we did not identify a bypass mechanism related to the activation of tyrosine kinase receptors (RTK) targeted by ponatinib by phospho-receptor tyrosine kinase (p-RTK) arrays (data not shown).

Western blot analysis in MR135-R1 showed that ALK inhibition with lorlatinib alone had no inhibitory effect on the phosphorylation of the downstream signaling pathways (**Fig. 4C**). Treatment of this cell line with vistusertib alone or in combination with lorlatinib inhibited S6 phosphorylation and increased the level of the proapoptotic BH3-only protein BIM and the proteolytic cleavage of PARP. This effect was more potent with the combination of vistusertib and lorlatinib. Similarly, the combination of lorlatinib and ponatinib reduced AKT, ERK, and S6 phosphorylation, and increased apoptosis as compared with either treatment alone (**Fig. 4C**).

To further assess the activity of the combined treatment against lorlatinib-resistant ALK-positive tumors *in vivo*, we examined the efficacy of lorlatinib and vistusertib against the corresponding MR135-R2 PDX. As shown in **Fig. 4D**, treatment of MR135-R2 PDX tumor-bearing mice with the combination was significantly more effective than with single agents in controlling tumor growth.

Independent validation of NF2 loss–mediated lorlatinib resistance

We performed *NF2* knock out (KO) by CRISPR-CAS9 gene editing in the ALK-rearranged H3122 cell line to further validate the implication of NF2 loss of function in lorlatinib resistance. The resulting H3122-NF2KO cell line harbored a genomic 22,803 bp deletion causing a 434 bp frameshift deletion at the mRNA level (Exon 4–12). Immunoblot analysis confirmed the lack of merlin expression in H3122-NF2KO cells (**Fig. 4E**).

Consistent with the MR135 cell lines, H3122-NF2KO cells were less sensitive to lorlatinib treatment than the parental cell line with an IC_{50} of 41.8 nmol/L compared with 1.3 nmol/L, respectively (**Fig. 4F**). The shift in the IC_{50} value was also observed for other ALK TKI (Supplementary Fig. S3F). We next assessed the magnitude of this effect in a time-course cell proliferation assay simultaneously with a caspase activity assay. H3122-NF2KO cells continued to proliferate in the presence of high doses of lorlatinib and exhibited low caspase activity

compared with the parental cell line at each time point (**Fig. 4G** and **H**). Western blot analysis revealed that merlin-deficient cells maintained higher levels of S6 phosphorylation compared with merlin-proficient cells (**Fig. 4I**). Consistently, with the caspase-3/7 activity assay, H3122-NF2KO cells had decreased levels of cleaved PARP after 48 hours of treatment with lorlatinib. Importantly, vistusertib alone or in combination with lorlatinib potently inhibited S6 phosphorylation and induced PARP cleavage in H3122-NF2KO cells (Supplementary Fig. S3G). This further supports the importance of merlin integrity in the regulation of mTOR signaling, evidenced by the overactivation of mTOR secondary to *NF2* knockout in this model (Supplementary Fig. S4).

Discussion

Lorlatinib, which has been recently granted FDA approval, is the new standard treatment for patients progressing after crizotinib and a second-generation ALK inhibitor or after upfront treatment with ceritinib or alectinib, and the last remaining available line of ALK-targeted therapy (6, 7, 23). With this study, we contributed to understand the adaptive mechanisms driving resistance to this targeted agent trough the longitudinal assessment of tumor biopsies and ctDNA by deep molecular profiling and the development of PDX and cell lines.

The sequential accumulation of mutations on a single allele of the *ALK* kinase domain has been recently described by Yoda and colleagues to mediate resistance in about 35% of patients previously exposed to first- and second-generation TKIs (8). In addition to these pivotal findings, we identified and characterized three novel compound mutations from patient tumor biopsies (F1174L/G1202R, L1196M/D1203N, and C1156Y/G1269A). The C1156Y/G1269A compound mutation retained sensitivity to lorlatinib both in Ba/F3 cells and the patient-derived cell line suggesting that cooccurring off-target mechanisms of resistance can drive disease progression even in the presence of compound mutations. Similarly to the previously described L1196M/G1202R mutation, the L1196M/D1203N mutation conferred high level of lorlatinib resistance. On the other hand, the G1202R/F1174L compound mutation resulted in a mild increase in resistance to lorlatinib compared with the single G1202R mutation, and is potentially targetable by increasing lorlatinib doses *in vitro*. However, this approach would not be feasible in patients, limited by the risk of increased toxicities. This is further supported by a recent study reporting the acquisition *in vitro* of the F1174L mutation arising from G1202R-mutant Ba/F3 cells, exposed to low doses of lorlatinib using ENU mutagenesis screening, conveying low levels of resistance to this drug (24). In this patient, the detection in ctDNA of multiple secondary ALK mutations, of which G1202R and S1206F were confirmed to be *in cis*, shows that compound mutations can be polyclonal events.

Our studies on patient-derived cell lines allowed to further explore off-target mechanisms of resistance to lorlatinib, contributing to past efforts in the design of novel therapeutic strategies (25). We developed two patient-derived cell lines that underwent EMT *in vitro* on treatment with lorlatinib involving SRC activation. EMT had previously been implied in resistance to ALK inhibitors and other targeted therapies in lung cancer (26–29). In addition, it is also known that SRC activation plays a key role in the development of EMT throughout different cancer types (30). Crystal and colleagues had previously reported that several ALK-resistant patient-derived cell lines were susceptible to combined ALK and SRC inhibition (25). In this study, we further demonstrated that this

association is highly effective in lorlatinib-resistant patient-derived cell lines undergoing EMT, and showed that SRC inhibition could partially restore E-cadherin expression in mesenchymal cells without completely reverting them to an epithelial phenotype. Interestingly, as recently shown for EGFR-mutant NSCLC, FGFR inhibitors sensitized ALK-rearranged EMT cell lines to lorlatinib *in vitro* (17). There are no effective therapies against lung cancer undergoing EMT; our work further supports the exploration of combination strategies in clinical trials for patients with off-target resistance mechanisms.

Finally, we identified NF2 loss of function as a novel bypass mechanism of resistance to lorlatinib (MR-135) and subsequently confirmed these findings *in vitro* by *NF2* knockout in the H3122 cell line. In this case, the NF2 splicing site mutation was present at the time of progression to crizotinib, and in this context, the patient experienced initial response to lorlatinib treatment. At the time of resistance, additional deleterious events in *NF2* occurred and led to a potent bypass mechanism. We hypothesize that NF2 loss of function was a functional convergence among multiple metastatic sites where sequential genomic events led to biallelic *NF2* deleterious mutations. The patient-derived cell lines were resistant to lorlatinib and sensitized by mTOR inhibition *in vitro* and *in vivo*, constituting a novel potential treatment approach in this context.

This study has several limitations, the first being the number of patients evaluable for resistance mechanisms and reported in this study. Among the 4 patients who achieved a partial response with lorlatinib, the PFS ranged from 3.7 (MR144) to 16 months (MR210) which seems shorter than reported in the phase II study of lorlatinib (7). Further studies are needed to disclose the full spectrum of resistance mechanisms to lorlatinib including from patients with prolonged benefit. Second, prelorlatinib tumor biopsies and plasma samples were not available in all cases, limiting the analysis of the impact of baseline genomic alterations in lorlatinib resistance. Third, during the development of patient-derived cell lines, the selective pressure introduced by passages *in vitro* and treatment exposure, may result in the outgrowth of more aggressive tumor cells and force the acquisition of EMT features.

In summary, the mechanisms of resistance to lorlatinib in patients with *ALK*-rearranged lung cancer can be diverse and complex. We have shown here that longitudinal tumor samplings combined with patient derived models can provide new insights on tumor dynamics and biological processes underlying disease progression, thereby, contributing to the design of novel therapeutic strategies.

Disclosure of Potential Conflicts of Interest

D. Planchard is an employee/paid consultant for AstraZeneca, Bristol-Myers Squibb, Boehringer Ingelheim, Celgene, Merck, Novartis, Pfizer, Prime Oncology, Peer CME, and Roche, and is an advisory board member/unpaid consultant for AstraZeneca, Bristol-Myers Squibb, Celgene, Merck, Novartis, Pfizer, Roche, and Boehringer Ingelheim. J.P. Thiery is an employee/paid consultant for BioSyngen Pte ltd, reports receiving other commercial research support from Enterprise Singapore, holds ownership interest (including patents) in Biocheetah Pte Ltd, and reports receiving other remuneration from Medicxi. K. Howarth is an employee/paid consultant for and holds ownership interest (including patents) in Inivata. O. Deas is an employee/paid consultant for XenTech. C. Naltet reports receiving speakers bureau honoraria from AstraZeneca. G. Vassal is an advisory board member/unpaid consultant for Pfizer. A.M. Eggermont is an employee/paid consultant for Ellipses, Forbion, Pfizer, and Novartis, and reports receiving speakers bureau honoraria from Biocad and MSD. J.-C. Soria is an employee/paid consultant for AstraZeneca, Astex, Clovis, GlaxoSmithKline, Gammamabs, Lilly, MSD, Mission Therapeutics, Merus, Pfizer, Pharmamar, Pierre Fabre, Sanofi, and Servier, and holds ownership interest (including patents) in AstraZeneca and Gritstone. B. Besse reports receiving

Authors' Contributions

Conception and design: G. Recondo, D. Planchard, G. Vassal, R. Bahleda, S. Michiels, A.M. Eggermont, F. Andre, K.A. Olaussen, J.-C. Soria, B. Besse, L. Friboulet
Development of methodology: G. Recondo, L. Mezquita, D. Planchard, R.L. Frias, R. Bahleda, L. Lacroix, J.-C. Soria, L. Friboulet
Acquisition of data (provided animals, acquired and managed patients, provided facilities, etc.): G. Recondo, L. Mezquita, F. Facchinetti, D. Planchard, L. Bigot, R.L. Frias, J.-Y. Scoazec, K. Howarth, O. Deas, J. Galissant, P. Tesson, F. Braye, P. Lavaud, L. Mahjoubi, R. Bahleda, A. Hollebecque, M. Ngo-Camus, L. Lacroix, C. Richon, N. Auger, T. De Baere, L. Tselikas, E. Angevin, F. Andre, C. Massard, B. Besse, L. Friboulet
Analysis and interpretation of data (e.g., statistical analysis, biostatistics, computational analysis): G. Recondo, L. Mezquita, F. Facchinetti, D. Planchard, A.Z. Rizvi, J.P. Thiery, J.-Y. Scoazec, K. Howarth, O. Deas, D. Samofalova, P. Tesson, R. Bahleda, S. Michiels, N. Auger, E. Angevin, K.A. Olaussen, B. Besse, L. Friboulet
Writing, review, and/or revision of the manuscript: G. Recondo, L. Mezquita, F. Facchinetti, D. Planchard, A. Gazzah, R.L. Frias, J.P. Thiery, J.-Y. Scoazec, T. Sourisseau, K. Howarth, C. Naltet, P. Lavaud, L. Mahjoubi, R. Bahleda, A. Hollebecque, S. Michiels, L. Lacroix, T. De Baere, L. Tselikas, E. Solary, E. Angevin, A.M. Eggermont, C. Massard, K.A. Olaussen, J.-C. Soria, B. Besse, L. Friboulet

Administrative, technical, or material support (i.e., reporting or organizing data, constructing databases): G. Recondo, L. Bigot, L. Mahjoubi, A.A. Lovergne, R. Bahleda, C. Nicotra, S. Michiels, L. Tselikas, E. Solary, E. Angevin, C. Massard, L. Friboulet
Study supervision: G. Recondo, A. Gazzah, G. Vassal, F. Andre, K.A. Olaussen, B. Besse, L. Friboulet

Acknowledgments

References

1. Hallberg B, Palmer RH. Mechanistic insight into ALK receptor tyrosine kinase in human cancer biology. Nat Rev Cancer 2013;13:685–700.
2. Dearden S, Stevens J, Wu Y-L, Blowers D. Mutation incidence and coincidence in non small-cell lung cancer: meta-analyses by ethnicity and histology (mutMap). Ann Oncol 2013;24:2371–6.
3. Koivunen JP, Mermel C, Zejnullahu K, Murphy C, Lifshits E, Holmes AJ, et al. EML4-ALK fusion gene and efficacy of an ALK kinase inhibitor in lung cancer. Clin Cancer Res 2008;14:4275–83.
4. Recondo G, Facchinetti F, Olaussen KA, Besse B, Friboulet L. Making the first move in EGFR-driven or ALK-driven NSCLC: first-generation or next-generation TKI? Nat Rev Clin Oncol 2018;15:694–708.
5. Zou HY, Friboulet L, Kodack DP, Engstrom LD, Li Q, West M, et al. PF-06463922, an ALK/ROS1 inhibitor, overcomes resistance to first and second generation ALK inhibitors in preclinical models. Cancer Cell 2015;28:70–81.
6. Shaw AT, Felip E, Bauer TM, Besse B, Navarro A, Postel-Vinay S, et al. Lorlatinib in non-small-cell lung cancer with ALK or ROS1 rearrangement: an international, multicentre, open-label, single-arm first-in-man phase 1 trial. Lancet Oncol 2017;18:1590–9.
7. Solomon BJ, Besse B, Bauer TM, Felip E, Soo RA, Camidge DR, et al. Lorlatinib in patients with ALK-positive non-small-cell lung cancer: results from a global phase 2 study. Lancet Oncol 2018;19:1654–67.
8. Yoda S, Lin JJ, Lawrence MS, Burke BJ, Friboulet L, Langenbucher A, et al. Sequential ALK inhibitors can select for lorlatinib-resistant compound ALK mutations in ALK-positive lung cancer. Cancer Discov 2018;8:714–29.
9. Massard C, Michiels S, Ferte C, Le Deley M-C, Lacroix L, Hollebecque A, et al. High-throughput genomics and clinical outcome in hard-to-treat advanced cancers: results of the MOSCATO 01 trial. Cancer Discov 2017;7:586–95.
10. Kodack DP, Farago AF, Dastur A, Held MA, Dardaei L, Friboulet L, et al. Primary patient-derived cancer cells and their potential for personalized cancer patient care. Cell Rep 2017;21:3298–309.
11. Friboulet L, Li N, Katayama R, Lee CC, Gainor JF, Crystal AS, et al. The ALK inhibitor ceritinib overcomes crizotinib resistance in non-small cell lung cancer. Cancer Discov 2014;4:662–73.
12. Plagnol V, Woodhouse S, Howarth K, Lensing S, Smith M, Epstein M, et al. Analytical validation of a next generation sequencing liquid biopsy assay for high sensitivity broad molecular profiling. PLoS One 2018;13: e0193802.
13. Li H, Durbin R. Fast and accurate short read alignment with Burrows-Wheeler transform. Bioinformatics 2009;25:1754–60.
14. Miller CA, White BS, Dees ND, Griffith M, Welch JS, Griffith OL, et al. SciClone: inferring clonal architecture and tracking the spatial and temporal patterns of tumor evolution. PLoS Comput Biol 2014;10:e1003665.
15. Dang HX, White BS, Foltz SM, Miller CA, Luo J, Fields RC, et al. ClonEvol: clonal ordering and visualization in cancer sequencing. Ann Oncol 2017;28: 3076–82.
16. Miller CA, McMichael J, Dang HX, Maher CA, Ding L, Ley TJ, et al. Visualizing tumor evolution with the fishplot package for R. BMC Genomics 2016;17:880.
17. Raoof S, Mulford IJ, Frisco-Cabanos H, Nangia V, Timonina D, Labrot E, et al. Targeting FGFR overcomes EMT-mediated resistance in EGFR mutant non-small cell lung cancer. Oncogene 2019;38:6399–413.
18. Avizienyte E, Frame MC. Src and FAK signalling controls adhesion fate and the epithelial-to-mesenchymal transition. Curr Opin Cell Biol 2005;17:542–7.
19. Katayama R, Shaw AT, Khan TM, Mino-Kenudson M, Solomon BJ, Halmos B, et al. Mechanisms of acquired crizotinib resistance in ALK-rearranged lung Cancers. Sci Transl Med 2012;4:120ra17.
20. Baser ME, Kuramoto L, Joe H, Friedman JM, Wallace AJ, Gillespie JE, et al. Genotype-phenotype correlations for nervous system tumors in neurofibromatosis 2: a population-based study. Am J Hum Genet 2004;75:231–9.
21. Cerami E, Gao J, Dogrusoz U, Gross BE, Sumer SO, Aksoy BA, et al. The cBio cancer genomics portal: an open platform for exploring multidimensional cancer genomics data. Cancer Discov 2012;2:401–4.
22. Petrilli AM, Fernandez-Valle C. Role of Merlin/NF2 inactivation in tumor biology. Oncogene 2016;35:537–48.
23. Shaw AT, Martini J-F, Besse B, Bauer TM, Lin C-C, Soo RA, et al. Efficacy of lorlatinib in patients (pts) with advanced ALK-positive non-small cell lung cancer (NSCLC) and ALK kinase domain mutations [abstract]. In: Proceedings of the American Association for Cancer Research Annual Meeting 2018; 2018 Apr 14–18; Chicago, IL. Philadelphia (PA): AACR; 2018. Abstract nr CT044.
24. Okada K, Araki M, Sakashita T, Ma B, Kanada R, Yanagitani N, et al. Prediction of ALK mutations mediating ALK-TKIs resistance and drug re-purposing to overcome the resistance. EBioMedicine 2019;41:105–19.
25. Crystal AS, Shaw AT, Sequist L V, Friboulet L, Niederst MJ, Lockerman EL, et al. Patient-derived models of acquired resistance can identify effective drug combinations for cancer. Science 2014;346:1480–6.
26. Gainor JF, Dardaei L, Yoda S, Friboulet L, Leshchiner I, Katayama R, et al. Molecular mechanisms of resistance to first- and second-generation ALK inhibitors in ALK-rearranged lung cancer. Cancer Discov 2016;6:1118–33.

27. Guo F, Liu X, Qing Q, Sang Y, Feng C, Li X, et al. EML4-ALK induces epithelial-mesenchymal transition consistent with cancer stem cell properties in H1299 non-small cell lung cancer cells. Biochem Biophys Res Commun 2015;459:398–404.

28. Kim HR, Kim WS, Choi YJ, Choi CM, Rho JK, Lee JC. Epithelial-mesenchymal transition leads to crizotinib resistance in H2228 lung cancer cells with EML4-ALK translocation. Mol Oncol 2013;7:1093–102.

29. Song K-A, Niederst MJ, Lochmann TL, Hata AN, Kitai H, Ham J, et al. Epithelial-to-mesenchymal transition antagonizes response to targeted therapies in lung cancer by suppressing BIM. Clin Cancer Res 2018;24:197–208.

30. Patel A, Sabbineni H, Clarke A, Somanath PR. Novel roles of Src in cancer cell epithelial-to-mesenchymal transition, vascular permeability, microinvasion and metastasis. Life Sci 2016;157:52–61.